Memory and correlation effects in the quantum theory of thermalization

H. S. Köhler
Physics Department, University of Arizona, Tucson, Arizona 85721
(Received 3 August 1995)

In a previous publication [H. S. Köhler, Phys. Rev. C **51**, 3232 (1995)] equilibration rates were studied for an extended system of nonequilibrium nuclear matter. The two-time Green's functions in the Kadanoff-Baym (KB) formalism were solved numerically. These quantum-mechanical calculations were compared with the Markovian (semi)classical Uehling-Uhlenbeck collision term often used in the analysis of collisions between heavy ions. The equilibration was found to be substantially slowed down by quantum effects. The theoretical as well as experimental study of nonequilibrium systems is of course of great interest in many areas of physics, e.g., within the realm of quantum transport in solid state devices. On the theoretical side various methods and approximations are the subject of intensive study. By the KB ansatz, for example, the equations can be simplified to a one-time kinetic equation while preserving the non-Markovian character. The generalized KB (GKB) ansatz of Lipavsky, Spicka, and Velicky [Phys. Rev. B **34**, 6933 (1986)] is often preferred. In this paper approximations based upon the GKB ansatz are discussed in relation to the exact KB formalism. Numerical comparisons are made for both the strongly interacting nuclear medium as well as an electron plasma. A non-Markovian collision integral, including memory effects in a quasiparticle approximation, is often discussed in the literature. It is found that this approximation appreciably overestimates the collision rates even more than the classical (Boltzmann) approximation. The inclusion of a width in the spectral function, i.e., going beyond the quasiparticle approximation, gives considerable improvement. The competition between the memory and correlation effects is found to lead to an anomalous saturation of the relaxtion rate.

PACS number(s): 05.30.−d, 05.20.Dd, 05.60.+w, 21.65.+f

I. INTRODUCTION

Results of numerical solutions of the Kadanoff-Baym (KB) equations for nonequilibrium nuclear matter were shown in a previous paper [1]. Comparisons were also made with classical Markovian dynamics. It is the purpose of the present paper to investigate further the validity of this and some other suggested reductions and approximations of the KB equations.

The study of nonequilibrium phenomena is an important subject in all branches of physics. In solid state physics one is concerned with the dynamics of charged particle plasmas in semiconductors and metals. In nuclear and high-energy physics the collision between composite particles, e.g., heavy ions, is another example. The theoretical study of these phenomena is almost exclusively based upon the Markovian transport equation already developed by Boltzmann. Corrections due to non-Markovian transport have been investigated to some extent. Starting with the work of Brueckner, another important question in the theory of transport has been greatly elucidated. This concerns the interaction used in the collision term. For weak interactions a Born approximation is assumed to be adequate. Thus, for charged particle interactions a screened (static or dynamic) Coulomb potential is customarily used. For stronger interactions, e.g., nuclear, a Brueckner type of effective interaction is in principle used. In practice this is too complicated and some simple approximation is used. To a first approximation one uses an interaction that reproduces scattering cross sections. As in the Coulomb case, one should, however, also include in principle dynamic effects by considering the medium and frequency (two-time) dependence of the interaction.

Correlations are explicitly neglected in the collision term in the classical Markovian-Boltzmann equation. The distribution functions relate in this case to freely propagating Green's functions. The kinetic energy is conserved in each binary collision. Consistent with these statements is the fact that the equilibrium solution of the Boltzmann equation is a Fermi distribution.

There is an increased interest in going beyond the Markovian Boltzmann equation. Effects of memory (i.e., non-Markovian effects) and correlations have been studied in various approximations. In previous works [1–3] the present author showed numerical comparisons between the quantum-transport theory of Kadanoff and Baym and the classical Boltzmann theory. The study was made with particular reference to collisions between heavy ions usually studied with the Boltzmann equation or the Boltzmann-Uehling-Uhlenbeck, Vlasov-Uehling-Uhlenbeck, etc., versions thereof. The general conclusion of the study was that quantum effects reduce relaxation rates by a factor as small as one-half.

In the present investigation it is sought to discuss sources of the quantum corrections in more detail. To do so it is found convenient to use the generalized Kadanoff-Baym (GKB) ansatz introduced by Lipavsky *et al.* [4]. This allows one to separate between the effects of time retardation and correlations.

The formalism and some technical details needed for the presentation are shown in Sec. II. This includes various approximations considered for the calculations, the results of which are shown in Sec. III. Results are shown both for a strongly interacting (nuclear) system (Sec. III A) and for a screened Coulomb (electron) system (Sec. III B). Section IV gives a short summary and some final conclusions.

II. FORMALISM

Only a short summary of the required formalisms is shown. For further details regarding the Kadanoff-Baym formalism see, for example, Refs. [5–7].

A. KB equations

In a homogeneous medium neglecting the mean field the KB equations reduce (with $\hbar=1$) to

$$\left(i\frac{\partial}{\partial t}-\frac{p^2}{2m}\right)G^{><}(\mathbf{p},t,t') = \int_{t_0}^{t} dt''[\Sigma^{>}(\mathbf{p},t,t'')-\Sigma^{<}(\mathbf{p},t,t'')]G^{><}(\mathbf{p},t'',t') - \int_{t_0}^{t'} dt''\Sigma^{><}(\mathbf{p},t,t'')[G^{>}(\mathbf{p},t'',t')-G^{<}(\mathbf{p},t'',t')], \tag{2.1}$$

$$\left(-i\frac{\partial}{\partial t'}-\frac{p^2}{2m}\right)G^{><}(\mathbf{p},t,t') = \int_{t_0}^{t} dt''[G^{>}(\mathbf{p},t,t'')-G^{<}(\mathbf{p},t,t'')]\Sigma^{><}(\mathbf{p},t'',t') - \int_{t_0}^{t'} dt''G^{><}(\mathbf{p},t,t'')[\Sigma^{>}(\mathbf{p},t'',t')-\Sigma^{<}(\mathbf{p},t'',t')]. \tag{2.2}$$

The notations are conventional. $G^{>}$ and $G^{<}$ are essentially the occupation numbers for holes and particles, respectively. The particle distribution function $f(\mathbf{p},t)$ is given by

$$f(\mathbf{p},t)=-iG^{<}(\mathbf{p},t,t). \tag{2.3}$$

The Green's functions $G^{>}$ and $G^{<}$ are related on the diagonal in the (t,t') plane by

$$G^{>}(\mathbf{p},t,t)=-i+G^{<}(\mathbf{p},t,t). \tag{2.4}$$

Also useful is

$$G^{>}(\mathbf{p},t,t')=[G^{>}(\mathbf{p},t',t)]^{*}. \tag{2.5}$$

The scattering rates Σ are given by

$$\Sigma^{><}(\mathbf{p},t,t')=-i\int\frac{d^3\mathbf{p_1}}{(2\pi)^3} \times\langle\tfrac{1}{2}(\mathbf{p}-\mathbf{p_1})|T^{>}(\mathbf{p}+\mathbf{p_1},t,t')|\tfrac{1}{2}(\mathbf{p}-\mathbf{p_1})\rangle \times G^{<>}(\mathbf{p_1},t',t). \tag{2.6}$$

Here $T^{>}$ is defined by

$$\langle\mathbf{p}|T^{>}(\mathbf{P},t,t')|\mathbf{p}\rangle=\int dt''dt'''d\mathbf{p}''d\mathbf{p}''' \times\langle\mathbf{p}|T^{+}(\mathbf{P},t,t'')|\tfrac{1}{2}(\mathbf{p}''-\mathbf{p}''')\rangle \times G^{>}(\mathbf{p}'',t'',t''')G^{><}(\mathbf{p}''',t'',t''') \times\langle\tfrac{1}{2}(\mathbf{p}''-\mathbf{p}''')|T^{-}(\mathbf{P},t,'''t')|\mathbf{p}\rangle. \tag{2.7}$$

The effective interaction $T^{\pm}$ is usually defined in a binary collision (ladder) approximation by an integral equation formally written as

$$T_{12}^{\pm}=V+VG_1^{\pm}G_2^{\pm}T_{12}^{\pm}, \tag{2.8}$$

where V is the "free" interaction potential. In the semiconductor case the bubble random-phase approximation summation is also important.

In the following $T^{\pm}$ will be approximated by a local time-independent effective interaction to be defined below. In the semiconductor calculation a statically screened Coulomb potential is used. The exchange term is not included. The equation (2.6) for the scattering rates then simplifies to

$$\Sigma^{><}(\mathbf{p},t,t')=-i\int\frac{d^3\mathbf{p}_1\mathbf{d}^3\mathbf{q}}{(2\pi)^6}V^2(\mathbf{q})G^{<>}(\mathbf{p}_1,t',t) \times G^{><}(\mathbf{q}+\mathbf{p}_1,t,t')G^{><}(\mathbf{p}-\mathbf{q},t,t'), \tag{2.9}$$

where V is the local interaction dependent on momentum transfer $\mathbf{q}$ only. The momentum inegrations are conveniently evaluated using the convolution theorem for Fourier transforms.

In previously published works the KB equations were solved numerically for nuclear matter initially in nonequilibrium [1–3]. The time evolvement of the distribution function, related to the Green's function by Eq. (2.3), was calculated from an initial distribution in momentum space described by two separated Fermi spheres. Results were presented with both an initially uncorrelated and an an initially correlated medium. In the latter case the time integrations described below were extended along the imaginary axis. All results in the present paper are with an initially uncorrelated medium.

The results in the previous works were expressed in terms of relaxation times as a function of density and the final equilibrated temperature. To accomplish this the Green's functions of the two times t and t' had to be time evolved (for each value of $\mathbf{p}$) in the (t,t') plane starting from $t=t'=t_0$, at which time the collisons are turned on. In other words, $G(t,t')$ was time stepped from t to $t\rightarrow t+\Delta t$ for all $t_0\leq t'\leq T$, where T is the present time and similarly for t'. The time integrations on the right-hand sides of Eqs. (2.1) and (2.2) require knowing the Green's functions for all times (points in time) within the square defined by $t_0\leq t\leq T$ and $t_0\leq t'\leq T$. The scattering rates $\Sigma(t,t')$ also need to be known for all times $t_0\leq t\leq T$, but only at $t'=T$ (and all times $t_0\leq t'\leq T$ at $t=T$). The numerical application of this formalism has in general been considered to be unfeasible, although one can find that under specific circumstances the computations can be made fairly simple. It was shown, for example, in the previous work for nuclear matter that the

memory time in that case was only a few fm/c so that only a few of the past times (mesh points in the time variable) had to be saved. It will be demonstrated below that this simplification is a consequence of the induced correlations in the medium.

Methods have been proposed with the purpose of reducing the two-time Green's function formalism to a simpler one-time theory. To this end approximations are sought that allow time stepping only along the diagonal $t=t'$. This requires seeking suitable approximations for the off-diagonal $G^<$ and $G^>$ needed in Eqs. (2.1) and (2.2). Relations have been proposed expressing the off-diagonal elements in terms of the diagonal. Using relations Eqs. (2.3) and (2.4), the formalism is then reduced to a one-time theory with one distribution function instead of the two coupled Green's functions $G^>$ and $G^<$.

In the following sections several such approximate formalisms are presented and tested numerically.

Approximations of the KB equations are suitably introduced with the help of the GKB ansatz.

This ansatz was introduced by Lipavsky *et al.* [4] and has some advantages over the earlier KB ansatz [5]. The GKB ansatz is given by

$$G^<(\mathbf{p},t,t')=G^<(\mathbf{p},t,t)S(\mathbf{p},t,t') \tag{2.10}$$

with $t'>t$ and

$$G^>(\mathbf{p},t,t')=G^>(\mathbf{p},t',t')S(\mathbf{p},t,t') \tag{2.11}$$

with $t>t'$, where S is the spectral function. In the exact solution of the KB equations the self-consistently calculated Green's functions are used when computing the collision kernel. In addition to these exact solutions, approximations will be shown in which various approximate Green's functions, based on the GKB ansatz, are used in the collision kernel. Two separate approximations of the spectral function will be considered: the quasiparticle and a Lorentzian, i.e., without and with a width.

B. Memory effect

In the quasiclassical approximation one has

$$S(\mathbf{p},t,t')=e^{i\omega(t-t')}. \tag{2.12}$$

One then simply obtains in this approximation, with t and t' ordered as in Eqs. (2.10) and (2.11), respectively,

$$G^<(\mathbf{p},t,t')=G^<(\mathbf{p},t,t)e^{i\omega(t-t')},$$

$$G^>(\mathbf{p},t,t')=[-i+G^<(\mathbf{p},t',t')]e^{+i\omega(t-t')}, \tag{2.13}$$

where we used Eq. (2.4) so that the off-diagonal elements $t\neq t'$ for both $G^>$ and $G^<$ are obtained simply from the $G^<$ on the diagonal.

The mean field is neglected in the present calculations and therefore $\omega=p^2/2m$. The main effect of the mean field is to reduce all relaxation rates with a factor equal to the effective mass.

Below we report on calculations in the above approximation for comparison with the "exact" KB results. These calculations are done with the same computer program as used for the KB calculations only modified by using the approximate Greens functions, given by Eq. (2.13), on the right-hand side of Eqs. (2.1), (2.2), and (2.6). It should be noted that as a consequence of the GKB ansatz the Green's functions $G^<$ and $G^>$ are now only needed at times (t,T) and (T,t'), respectively, related to the time diagonal by Eq. (2.13). The computation is reduced to a time stepping along the diagonal only as in a one-time kinetic equation. In the presentation of numerical results below, this approximation will be referred to as the *memory effect*.

It is easy to see that in the above *memory* approximation the collision integral indeed reduces to the well-known kinetic equation including memory effect. In fact, we see that using the approximate Greens functions given by Eq. (2.13) on the right-hand side of Eq. (2.1) and using Eq. (2.3), one obtains

$$\frac{\partial}{\partial t}f(\mathbf{p},T)=\int\frac{d^3\mathbf{p}_1d^3\mathbf{p}'d^3\mathbf{p}'_1}{(2\pi)^6}\int_{t_0}^{T}dt\,2\cos[(\omega+\omega_1-\omega'-\omega'_1)\times(T-t)]V^2(\mathbf{p}-\mathbf{p}')(FF_1f'f'_1-ff_1F'F'_1)\delta(\mathbf{p}+\mathbf{p}_1-\mathbf{p}'-\mathbf{p}'_1), \tag{2.14}$$

with $f\equiv f(\mathbf{p},t)$ and $F\equiv 1-f$, etc. This is the familiar non-Markovian extension of the Boltzmann collision term including a memory effect but neglecting the effects of the width Γ, i.e., the induced correlations. In this approximation there is still an integration over past times as in the original Kadanoff-Baym equations, but there is an appreciable reduction in computational effort as the Green's function (or distribution function) only has to be known and time evolved along the diagonal times $t=t'$.

The integration over past times is evidently important only if the relaxation time is short compared to the memory time itself and this has been demonstrated in several calculations [8–11]. In equilibrium the distribution function is constant and if the integration is extended over all times the time integration results in a δ function of the energies as in the classical equation. The quantum effect contained in the retardation is therefore seen to be related to the energy broadening due to the time rate of change of the system, but not to the correlations between particles. The memory effect results in nonconservation of kinetic (single-particle) energies, as seen from Eq. (2.14).

C. Memory effect with damping

Starting with a noninteracting system, in which case the spectral function has zero width, and turning on the interactions, subsequent collisions between the particles result in a nonzero width of the spectral function, i.e., there is a buildup of correlations. In previous work initially correlated Green's functions were also used following work by Danielewicz [7,12]. It was found to be important to include this effect especially at low temperatures (excitations). In the present work we introduce the effect approximately by introducing a constant and finite width in the spectral function. Thus

$$S(\mathbf{p},t,t')=e^{-(1/2)\Gamma(t-t')}e^{i\omega(t-t')}, \tag{2.15}$$

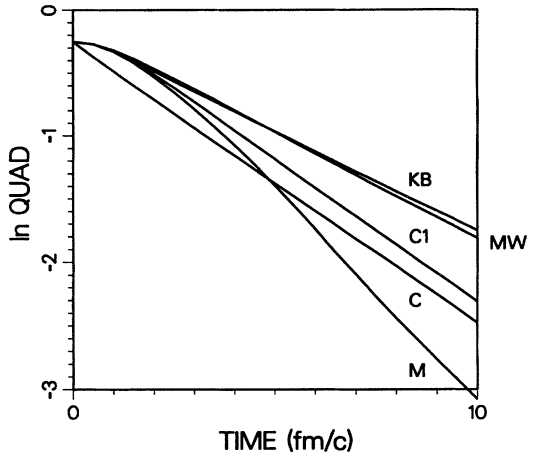

FIG. 1. Logarithm of the quadrupole moment of the distribution in momentum space as a function of time, for nuclear matter of normal density excited to 45 MeV. The curves are marked as follows (for more details see the text): KB, two-time Green's functions; C, classical; $C1$, modified classical; M, memory; MW, memory with damping (width).

i.e., a Lorentzian distribution with Γ being the width. This width is directly related to the correlation time $t_{\rm corr}$ by

$$\Gamma=\hbar/t_{\rm corr},$$

where $t_{\rm corr}$ is defined as the time for the system to become correlated. This time can be identified in the KB calculations as the time at which the correlation energy becomes constant (see, for example, Fig. 2 in Ref. [1]). Because of the finite width the integrations over past times will be cut off with $\Gamma>0$, therefore reducing the memory time and the collision rates. Numerical results in this approximation will be presented below and will be referred to as calculations of the *memory effect with damping*. The damping is simply included in Eq. (2.14) by a factor $e^{-2\Gamma(T-t)}$ in the integrand [13].

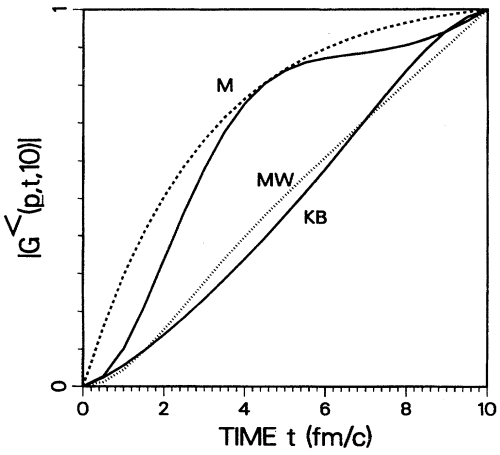

FIG. 2. Absolute value of the two-time Green's function $G^<(\mathbf{p},t,t')$ with $\mathbf{p}=0$. Off-diagonal elements in (t,t') is shown with t' fixed at 10 fm/c.

D. Classical approximation

A characteristic of the KB equations that is also maintained in the equations with memory effect is that kinetic energy is not conserved in the collision between the two particles, i.e., a typical many-body quantum effect. The energy broadening is directly related to the relaxation time as follows. In the limit of a static (equilibrium) system the memory effect ceases to be relevant and the Boltzmann limit is obtained. This is easily seen from Eq. (2.14); in equilibrium the distribution function is constant and if the integration is extended over all times the time integration results in a δ function of the energies ω. The (kinetic) energy is conserved in each binary collision and therefore also globally. This limit is also obtained by *approximating* the Green's functions on the right-hand side of Eq. (2.13) by values at time T, i.e., the present time. Thus

$$G^<(\mathbf{p},t,T)=G^<(\mathbf{p},T,T)e^{i\omega(t-T)},$$

$$G^>(\mathbf{p},T,t')=[-i+G^<(\mathbf{p},T,T)]e^{i\omega(T-t')}, \quad (2.16)$$

where the time T is, as before, the present time. The classical calculations presented below were made with the KB computer program, but with the Green's functions in the collision kernel approximated by the above equation (2.16).

In this case the time integration in Eq. (2.14) can of course be performed analytically and *if* extended over all times it yields a δ function expressing the conservation in kinetic energy in each binary collision and therefore also globally. The classical Boltzmann equation is thus obtained.

A comparison of the KB results with the classical Boltzmann equation was one of the main topics of the previous publications in this series [1–3]. The numerical results for the classical case were then obtained from a completely different computer program that explicitly contained the δ function over kinetic energies referred to above. In the present paper classical results will again be shown. But we stress again that they are now obtained by modifying the KB program, following the discussion above, by approximating the Green's functions in Eqs. (2.1), (2.2), and (2.6) by Eq. (2.16). In addition, the time integration is extended over sufficiently long (negative) times that the δ function of the energies is well approximated. Details of this (and other parts of the calculation) are described below.

If, however, the time integration is maintained within the limits t_0 and T there is still an energy broadening. This broadening is directly related to the time range of the integration, i.e., to the time the system is "observed." It is therefore expected to deviate from the classical at the beginning of the evolution when the time interval is short. This broadening is in fact present in all the calculations (except for the initially correlated), i.e., in the case of the full quantum as well as in the approximate, at the beginning of the respective evolutions. To isolate this effect, results will be shown for both ranges of time integrations, i.e., the extended and the finite, t_0 to T.

The energy broadening due to the short observation time can also be avoided by starting the time integrations in the quantum and the other approximations at some time less than t_0, i.e., before the collisions are switched on. Such calculations were also made, but results of these are not shown here.

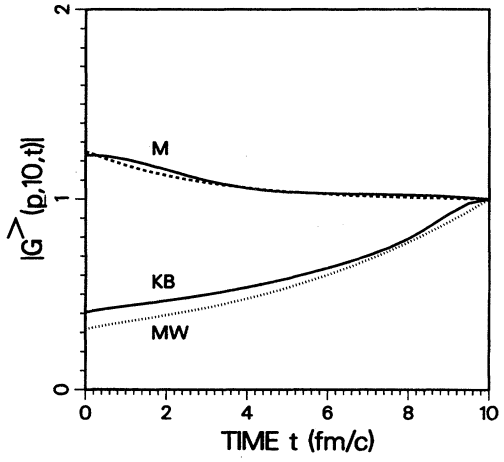

FIG. 3. Similar to Fig. 2, except that this is for the Green's function $G^{>}$.

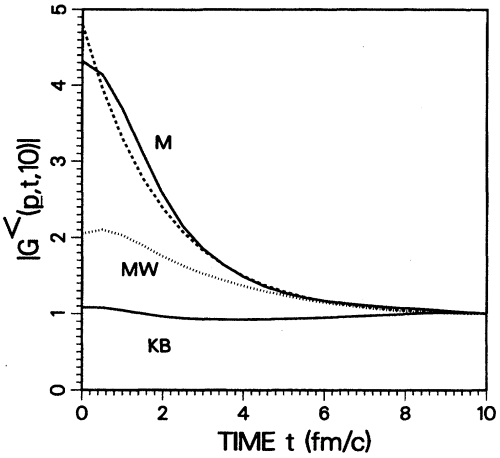

FIG. 4. Similar to Fig. 2, except that $p=1.2$ fm^{-1} and this is on the symmetry axis.

It should be pointed out that in these cases (i.e., other than the classical) correlations are induced, so that the system is excited above the initial state. This is avoided by the imaginary time stepping used in a previous paper [1].

III. NUMERICAL RESULTS

The numerical results presented in this paper are primarily aimed at testing the various approximations decribed above. We believe that these tests are particularly meaningful because all the calculations are made with essentially the same computer program as explained in Sec. II, so that numerical uncertainties due to meshes, etc., are minimized. Results are presented for both nuclear matter and semiconductors.

A. Nuclear results

The nuclear calculations are done with the same meshes as used in Ref. [1]. The approximations of the present paper is tested for the case of a final equilibrated temperature of 45 MeV and normal density. The initial distribution is as in the earlier calculations, that of two separated Fermi spheres. In this case the Fermi momentum of each sphere is 1.1041 fm^{-1} and the centers are separated by 3.383 fm^{-1}. Consequently, the surfaces of the two spheres are separated by ~ 1.2 fm^{-1} and the density betwen them is zero. This is important for the understanding of Figs. 2–5. Results of the KB calculations for this particular case are shown both for a correlated and for an uncorrelated initial distribution in Fig. 5 of [1]. The classical result is also shown in the same figure. The figure is a logarithmic plot of the quadrupole moment of the distribution function as a function of time.

In Fig. 1 of the present paper the curve marked KB shows the same KB result with an initial uncorrelated distribution, while curve C is the classical result. This latter result is also identical to that shown in Fig. 5 of [1]. It is now calculated, however, as described in Sec. II D, with $t_0=-10$ fm/c. The kinetic energy was then essentially constant, increasing slightly from an initial 74.1 to 74.6 MeV/A at the end of the run. The curve $C1$ shows the result of energy broadening; the classical calculation is modified by restricting the time integration as described above by choosing $t_0=0$. The kinetic energy is, in this case, increasing from 74.1 to 110.0 MeV/A, reached to within 2% at $t=5$ fm/c. It is seen that curves $C1$ and KB overlap during the initial correlation time, while at later times C and $C1$ become nearly parallel. The range of the time integration for $C1$ is then large enough to reduce the energy broadening so that C and $C1$ show the same slope.

Curve M in the same figure shows the memory effect. In this case the kinetic energy saturates at about 103 MeV/A at $t=5$ fm/c. It is seen that this approximation deviates even more from the KB result than does the classical approximation. Further inspection of the calculations discussed below in relation to Figs. 2–5 shows a simple explanation. The integration over past times enhances the collision rates because at the past times the deviation from equilibrium is much larger. The equilibration follows a decay law that is almost exactly exponential. The memory effect therefore greatly exaggerates the contribution from past collisions. The quasiclassical spectral function [Eq. (2.12)] that was used in

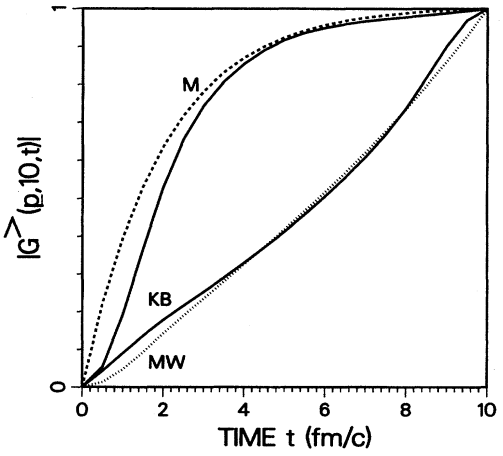

FIG. 5. Similar to Fig. 3, except that $p=1.2$ fm^{-1} and this is on the symmetry axis.

deriving this approximation neglects the width present in the exact KB theory. This width acts as a cutoff in the time integration. It is included in the approximation referred to above as a memory effect with damping. The curve labeled MW in Fig. 1 shows the result of such a calculation, with a constant width of 50 MeV, showing near agreement with the KB result.

To further illustrate the nature of the various approximations, absolute values of the off-diagonal elements of $G^>$ and $G^<$ in (t,t') space are plotted in Figs. 2–5. They are all normalized to the value one at 10 fm/c. One of the time arguments is as indicated, chosen to be 10 fm/c. The curves are labeled as in Fig. 1. The Green's functions for the classical Markovian approximation are not plotted. They will be constant and equal to the value one for all times.

Figures 2 and 3 show the results for the momentum $p=0$. The occupation of momentum states is here equal to zero at the initial time $t=0$ and consequently $G^<(p=0,0,10)=0$ in Fig. 2. As $T\to\infty$ an equilibrium will eventually be reached. The diagonal (equal times) elements of $G^<$ follow closely an exponential law, i.e., $G(0,t,t)\sim 1-e^{-t/\tau_{\rm rel}}$. By Eq. (2.13) the memory approximation, i.e., the solid curve M in Fig. 2, also follows roughly this exponential law shown by the dotted line M with $\tau_{\rm rel}=3$ fm/c, which is the final relaxation time for the quadrupole moment in the memory calculation, as can be seen from Fig. 1. It is, however, also seen from Fig. 1 that the relaxation time is not really constant in this case and therefore the solid and dotted curves M in Fig. 2 do not overlap that well. This is especially obvious for the first few fm/c when the system is still being correlated and all relaxations are slower. It should also be noted that the system has not yet reached equilibrium at $t=10$ fm/c. In the case of memory effect with damping the exponential factor in Eq. (2.15) supresses the solid line M to the dotted line MW, which agrees quite well with the exact KB result shown by a solid line.

The corresponding results for $G^>$ are shown in Fig. 3. In the memory approximation the Green's function $|G^>(p=0,10,t=0)|=1$ and it will decay with increasing t. The solid curve marked M shows the result in this approximation normalized to the value one at $t=10$ fm/c. The dotted curve M shows the result, as in Fig. 2, if the relaxation were to follow an exponential decay with a relaxation time $\tau_{\rm rel}=3$ fm/c. Comparing with the KB result (shown by the solid line KB), one finds again that the approximation M therefore greatly exaggerates the past values of $G^>$, while suppression due to the damping brings the result close to the KB result, as shown by the dotted curve marked MW.

Figures 4 and 5 show the corresponding results for $G^<$ and $G^>$, respectively, at a momentum $p=1.2$ fm^{-1} along the symmetry line of the distribution, i.e., at a point that lies inside one of the initial Fermi spheres so that this state is then fully occupied. The memory calculation of $G^<$ is shown by the solid line marked M in Fig. 4. It is here found that it is fitted with a relaxation time 2 fm/c, i.e., somewhat smaller than the 3 fm/c found for the states at the center of momentum space. The deviation from the KB curve is here significant, again showing that the memory effect exaggerates the contribution from past times. The constant correlation (damping) width $\Gamma=50$ MeV used in the calculations is too

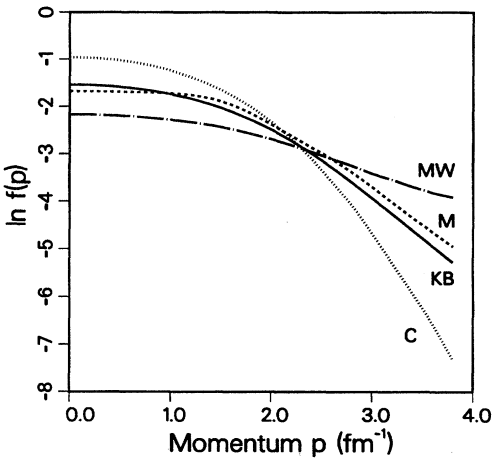

FIG. 6. Logarithm of the distribution function shown in various approximations along an axis perpendicular to the symmetry axis and with $p_\parallel=0$ and at $t=10$ fm/c.

small at this momentum state, as shown by the curve marked MW, but it gives a substantial improvement over the M curve. The corresponding result for $G^>$ in Fig. 5 shows, however, that the damping is sufficient in this case.

An important quantum effect already pointed out by Danielewicz [7] is that particles will occupy the high momentum states more quickly than in the classical case. This is a consequence of the nonconservation of energy in individual collisions in the quantum case as opposed to the classical. This situation is illustrated by Fig. 6 for the various approximations under consideration here. This figure shows a logarithmic plot of the distribution functions for particles scattered into states perpendicular to the beam axis and with $p_\parallel=0$ at $t=10$ fm/c. The result shows, as noted above, that the classical approximation greatly underestimates the distribution function for $p>2.5$ fm^{-1}. Somewhat surprising is that the memory effect shows a good result here, while the memory effect with a width gives too large values.

A final example of the effect of correlations is shown in Fig. 7. Here the initial distribution is a zero-temperature Fermi sphere. In the KB case correlations build up with final occupation numbers shown by the full line. The initial kinetic energy of the uncorrelated Fermi distribution is 24 MeV/A and after a few fm/c it increases, because of the correlations to 48 MeV/A. This was already shown by Fig. 2 in Ref. [1]. The memory calculation is shown by the broken line. The kinetic energy rises in this case to a larger value, 55 MeV/A. Correlations are stronger and the depletion of states is larger. The larger correlations in the memory calculations are thus consistent with the results above.

B. Semiconductor results

In semiconductors one may have one or two component plasmas that can be produced either optically or by means of doping. The effective masses are determined by the band structure. We concentrate here on a one-component plasma. In this case the interaction is the screened Coulomb potential. The optical excitations result in plasmas that are deformed in momentum space. The actual shape of this defor-

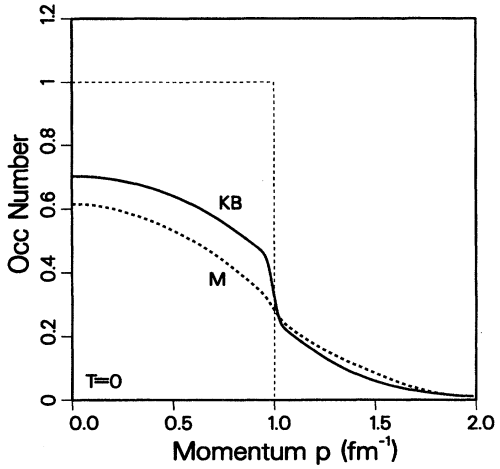

FIG. 7. Effect of correlations for the quantum case (KB) and in the memory approximation (M). The initial uncorrelated distribution is shown by a broken line with ocupation-numbers being 1 and 0.

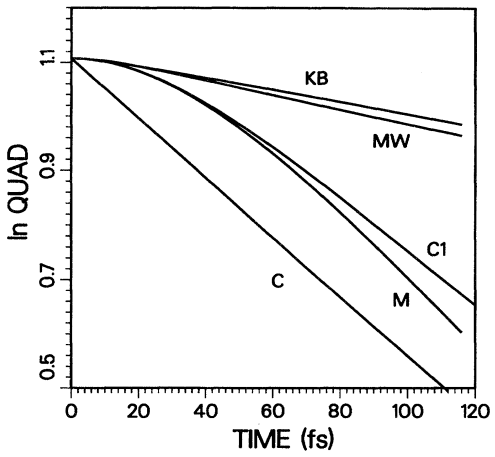

FIG. 8. Similar to Fig. 1, except that this is for an electron plasma. The initial distribution is defined in the text. The screening length is $\kappa=0.2a_B^{-1}$.

mation depends on the details of the semiconductor. In this exploratory calculation we simply choose as an initial distribution two Fermi spheres, like in the nuclear matter case, but here they are both heated to a temperature of $T=228$ K with a Fermi energy $\mu=0$. The distance between the centers of the two Fermi spheres is $2.0a_B^{-1}$ and the total density is then 0.708 electrons/a_B^3 with the Bohr radius $a_B^{-1}=132$ Å. The effective mass is taken to be $0.067m_e$. These are representative values for an electron-plasma in semiconductors [14]. The screening length κ of the Coulomb potential is varied between $0.2a_B^{-1}$ and $1.0a_B^{-1}$. For comparison, the static screening length was calculated to be $\kappa\sim 1.5a_B^{-1}$.

As a measure of the momentum relaxation, the quadrupole moment of the distribution was calculated as a function of time, as it was for nuclear matter. The results for the approximations under consideration are plotted in Fig. 8. Comparing with the nuclear calculations in Fig. 1, it is seen that in both cases the KB calculation relaxes slower. The MW calculation is almost the same, with the damping taken to be $\Gamma=0.025$ eV in the atomic case. In the nuclear case the memory effect has a much faster relaxation than all the others. In the atomic calculation this, however, is not so. It rather agrees with the $C1$ calculation. After initial correlations the relaxation rates of C and $C1$ are very much the same as in the nuclear case. This shows that in this case the memory effect is relatively small and that the effect of correlations is the dominant factor. The difference between the KB and C calculations are much larger in the atomic case than in the nuclear case. As shown in an earlier publication [1], this difference depends, however, on the temperature and the results are therefore not comparable.

A characteristic of all but the Boltzmann calculation is the increase of kinetic energy as correlations develop from an initially uncorrelated system. The initial kinetic energy for the chosen distribution is $6.74E_R/a_B^3$. At the end of the calculations we find, respectively, for KB, 8.59; M, 8.28; MW, 8.85; and $C1$, $6.89E_R/a_B^3$. The C calculation (Boltzmann) was made with t_0 chosen to be -160 fs and the final kinetic energy was then $6.75E_R/a_B^3$, i.e., very well conserved. The Rydberg energy is here $E_R=4.2$ meV.

The screening length κ is not only density dependent but it is a kinetic variable [15]. The value chosen in Fig. 8 is relatively small. As the screening length increases and the interaction decreases in strength it is expected that all the different approximations would converge to a common result. This is illustrated by Fig. 9, where $\kappa=1a_B^{-1}$ instead of $\kappa=0.2a_B^{-1}$, as in Fig. 8. As expected, the classical (C) and memory (M) calculations both show a decreased relaxation rate. Surprising, however, is that the quantum calculation (KB) approaches those curves as a result of a *increased* relaxation rate. The situation is further illustrated by Fig. 10. The relaxation time for the quantum evolution (curve marked KB) is shown as a function of the screening length κ. The

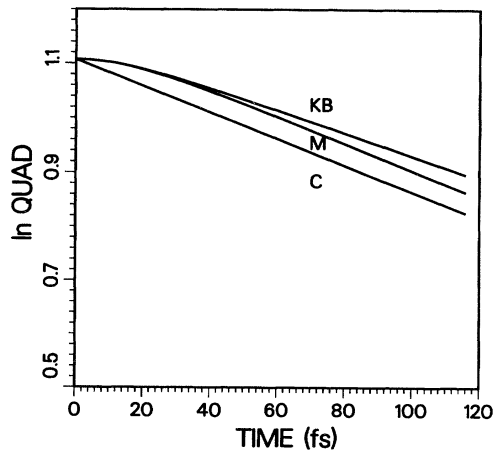

FIG. 9. Similar to Fig. 8, except that here $\kappa=1.0a_B^{-1}$.

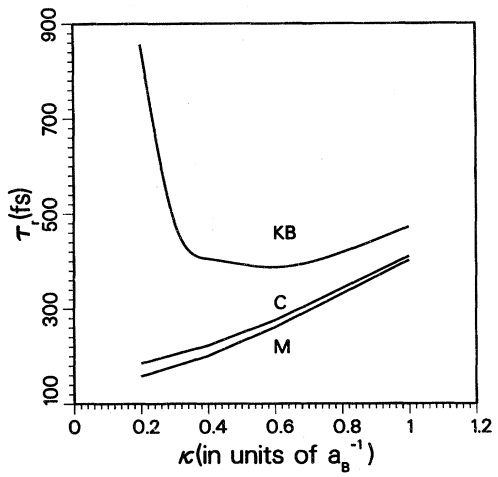

FIG. 10. Relaxation time τ_r is plotted as a function of screening length κ. Note the saturation of relaxation as the strength is increased (κ decreased) in the quantum calculation (KB). This anomaly is not seen in the memory (M) nor (of course) in the classical calculation (C).

strength of the interaction increases with decreasing κ. One would therefore expect the relaxation time to decrease as κ is decreased. Instead one finds a saturation point at $\kappa \sim 0.6$. The curves marked C and M for the classical and memory calculations, respectively, show, on the other hand, the expected behavior as a function of κ. Figure 10 also shows, as pointed out earlier, that the memory calculation gives a somewhat shorter relaxation time relative to the classical calculation.

The above discussion refers to the relaxation time of the quadrupole moment of the distribution function. The same anomaly is seen to occur also for the relaxation of the radial distribution function by comparing Figs. 1(d) and 2(d) of Ref. [14].

The anomaly can rather easily be understood from our previous results. It has been seen that the memory effect alone tends to increase the relaxation rate, while the correlations leads to a decrease. The competition between these two effects can, under the right circumstances, lead to the described anomalous saturation effect. In the classical case the rate scales of course simply with the square of the strength.

IV. SUMMARY AND CONCLUSIONS

Previous comparisons between the quantum and classical relaxation rates in nuclear equlibrations are extended to comparisons also with relaxation rates calculated including only memory effects but excluding the correlations. The memory effect calculations were also extended by an approximate inclusion of the damping of memory due to the correlations. It is found that memory-effect alone overestimates the retardation effects. The approximate damping effect showed appreciable improvement in comparison with exact Kadanoff-Baym quantum collisions. The agreement and disagreement with the KB results were shown to be directly related to the off-diagonal behavior of the Green's functions in the various approximations.

The approximations were formally obtained from the KB equations by using the GKB ansatz. In the quasi-particle approximation the memory approximation (M) was obtained. Allowing a width in the spectral function due to correlations, the approximation referred to as memory with damping (MW) was obtained. Neglecting both memory and width, the classical approximation (C or $C1$) was obtained.

The initial correlated distributions that were generated in the nuclear case in the previous nuclear calculations [1] have so far not been considered in the atomic case. Because of the weaker interactions the correlation times $t_{\rm corr}$ are in the latter case relatively longer and it is expected that a larger number of time steps along the imaginary axis will be required. The small width of the spectral function in ω space transforms to a large width in (t,t') space in the atomic case. It is quite feasible to do the calculations for a strongly interacting system in (t,t') space. For weakly interacting systems it may be more feasible to do the calculations in ω space.

The calculations presented here were made possible by using a local interaction when evaluating the collision term. This allowed the use of a fast Fourier transform routine for this calculation. The exact KB calculation is then no more time-consuming than the approximate ones. It would, however, be desirable for both nuclear and atomic problems to extend the calculations to include exchange nonlocal potentials.

The present comparisons of approximations show that both memory and correlation effects have to be included for reliable estimates of equilibrations. In the calculations presented here the exact KB calculations were no more difficult than the approximate ones. For extensions to more realistic interactions, etc., one may, however, have to seek suitable approximation methods. The present work may be helpful also in this endeavor.

The effects of memory and correlations are often opposed. The former tends to increase the rate of the evolution while the latter slows it down. This can lead to an interesting anomaly, as discussed in relation to Fig. 10.

The same competition between memory and correlation, is also believed to explain why the classical and quantum widths displayed in Fig. 6 of Ref. [1] converge at the high-temperature end of that figure. The memory effect increases with temperature as the relaxation rate increases and the past distribution becomes increasingly different from the present. The effect of correlation [Γ in Eq. (2.14)] stays essentially constant however. The net result is that correlations will therefore dominate the evolution at low temperature while the memory effect will take over at higher temperature. The anomalous scaling of the relaxation rate with the strength of the interaction is of course a consequence of the nonlinear structure of the quantum equations already pointed out by Danielewicz (see Fig. 8 of Ref. [7]).

ACKNOWLEDGMENTS

It is a pleasure to thank Professor Rolf Binder for the many discussions and for his critical comments on the manuscript, especially as regards the electron plasma calculations. I also wish to thank Dr. Michael Bonitz for a careful reading of the manuscript and for suggesting several corrections. This work was supported in part by the National Science Foundation Grant No. PHY-9407146.

[1] H.S. Köhler, Phys. Rev. C **51**, 3232 (1995).
[2] H.S. Köhler, Nucl. Phys. A **583**, 339 (1995).
[3] H.S. Köhler, in *Proceedings of the Seventh International Conference on Nuclear Reaction Mechanisms, Varenna, 1994*, edited by E. Gadioli (Universita degli Studi di Milano, Milano, 1994).
[4] P. Lipavsky, V. Spicka, and B. Velicky, Phys. Rev. B **34**, 6933 (1986).
[5] L.P. Kadanoff and G. Baym, *Quantum Statistical Mechanics* (Benjamin, New York, 1962).
[6] W.D. Kraeft, D. Kremp, W. Ebeling, and G. Röpke, *Quantum Statistics of Charged Particle Systems* (Akademie-Verlag, Berlin, 1986); D. Kremp, W.D. Kraeft, and A.J.D. Lambert, Physica A **127**, 72 (1984).
[7] P. Danielewicz, Ann. Phys. (N.Y.) **152**, 305 (1984).
[8] C. Greiner, K. Wagner, and P.-G. Reinhard, Phys. Rev. C **49**, 1693 (1994).
[9] S. Ayik and M. Dworzecka, Nucl. Phys. A **440**, 424 (1985); S. Ayik and J. Randrup (unpublished).
[10] K. Morawetz, R. Walke, and G. Roepke, Phys. Lett. A **190**, 96 (1994).
[11] K. Morawetz and G. Roepke, Phys. Rev. E **51**, 4246 (1995).
[12] P. Danielewicz, Ann. Phys. (N.Y.) **152**, 239 (1984).
[13] D.B. Tran Thoai and H. Haug, Z. Phys. B **91**, 199 (1993).
[14] M. Bonitz, D. Kremp, D.C. Scott, R. Binder, W.D. Kraeft, and H.S. Köhler (unpublished).
[15] R. Binder and S.W. Koch, Prog. Quantum. Electron. **19**, 307 (1995).